Available online at www.sciencedirect.com
ScienceDirect
Russian Geology and Geophysics 49 (2008) 877–881
RUSSIAN GEOLOGY AND GEOPHYSICS
www.elsevier.com/locate/rgg

TEM-TDEM soundings in the eastern Siberian craton

G.M. Morozova *, E.Yu. Antonov

Trofimuk Institute of Petroleum Geology and Geophysics, Siberian Branch of the RAS, 3 prosp. Akad. Koptyuga, Novosibirsk, 630090, Russia

Received 14 September 2007; accepted 31 January 2008

Abstract

We report forward modeling results for transient magnetic fields excited by horizontal electric or vertical magnetic dipoles. Modeling was performed with reference to resistivity patterns typical of platform areas in East Siberia. We investigate the possibilities to resolve deep reservoirs by measuring the horizontal and vertical components of the transient magnetic field and compare the depth resolution of magnetic and inductive methods.

Keywords: Transient electromagnetics; mathematical modeling; transient magnetic field

Introduction

Most of proven reserves in the East Siberian petroleum province occur in deep Late Proterozoic or Paleozoic reservoirs. They are, for instance, Late Proterozoic and Early Cambrian oil and gas fields discovered in Yakutia and Irkutsk region (Mandel'baum et al., 1980), several small subeconomic plays in the Irkutsk region (Yarakta, Bratsk, Markovo, Ayan, Nepa), the developed Kovykta and Khanda (Toropov and Man'kovskii, 2004) or Middle Botuobia and Upper Vilyuchansk gas fields in Yakutia. However, the deeper and the older the reservoirs the less they are explored.

The sedimentary cover of the Siberian Platform consists mainly of resistive carbonate rocks (Mandel'baum et al., 1980) with an average resistivity of 50–100 Ohm·m. The Cambrian strata, however, bear brines with a salinity above 300–400 g/l and resistivities much lower than in the host rocks. The resistivities of sandstones vary from 0.3 to 5 Ohm·m as a function of porosity (from 10 to 20%) and temperature (10 to 50 °C) (Mandel'baum et al., 1980). The sharp resistivity contrast (up to 100 times) between the formation water and the rocks is used as a physical background in detecting oil and gas reservoirs.

Near-field TEM soundings are known to be highly sensitive to the electrical conductivity of the subsurface (Kaufman, 1971; Kaufman and Morozova, 1970). The method has been updated lately due to advanced facilities of data acquisition and processing, to a broad use of GPS, and to new measurement systems. Much of progress in measurement techniques has been achieved with modifications of the *Impuls* (designed by G.M. Trigubovich) and *Tsikl* (Russian for *cycle*) (designed by B.P. Balashov and A.K. Zakharkin) systems and with new systems of TEM-FAST (designed by P.O. Barsukov and E.B. Fainberg) or SGS-TEM (designed by A.V. Pospeev and S.M. Stefanenko). For details of design and applications of the new TEM techniques see (Agafonov, 2005; Agafonov and Pospeev, 2001; Barsukov et al., 2002; Epov et al., 1990; Epov and Yel'tsov, 1992; Kondrat'ev et al., 2004; Trigubovich et al., 1990; Zakharkin, 1981).

However, the currently practiced noncoincident-loop TEM measurements cannot fully benefit from all advantages of in-line and array acquisition. The components of the TEM field are either independent of or proportional to the transmitter-receiver separation at late times (Kaufman, 1971; Kaufman and Morozova, 1970). See Table 1 for these relationships in the case of two-layer resistivity patterns with a conductor or an insulator at the base.

Here M is the moment of the magnetic dipole, Ix is the moment of the electric dipole, σ_2 is the conductivity of the base, $S = \sigma_1 h$ is the layer longitudinal conductance, $\mu_0 = 4\pi \cdot 10^{-7}$ H/m is the magnetic permeability, and φ is the azimuth.

It follows from the equations that the magnetic components H_x and H_z of the TEM field excited by an electric dipole are proportional, at late times, to r^2 and r and to the fourth and third power of conductance (S^4 and S^3), respectively. The radial component H_r of the magnetic dipole is proportional to the separation and to the fourth power of conductance (S^4).

* Corresponding author.
E-mail address: MorozovaGM@ipgg.nsc.ru (G.M. Morozova)

1068-7971/$ - see front matter © 2008, IGM, Siberian Branch of the RAS. Published by Elsevier B.V. All rights reserved.
doi:10.1016/j.rgg.2008.01.010

Table 1

Transmitter: horizontal electric dipole	
Base-conductor	Base-insulator
$H_x = \frac{I_x r^2 \sin 2\varphi}{1024\pi}\left(\frac{\sigma_2\mu_0}{t}\right)^2$	$H_x = \frac{I_x r^2 \sin 2\varphi}{16\pi}\left(\frac{\mu_0 S}{t}\right)^4$
$H_z = \frac{I_x r \sin\varphi}{60\pi\sqrt{\pi}}\left(\frac{\sigma_2\mu_0}{t}\right)^{3/2}$	$H_z = \frac{I_x r \sin\varphi}{32\pi}\left(\frac{\mu_0 S}{t}\right)^3$
Transmitter: vertical electric dipole	
$H_z = -\frac{M}{2\pi\cdot 15\sqrt{\pi}}\left(\frac{\sigma_2\mu_0}{t}\right)^{3/2}$	$H_z = -\frac{M}{16\pi}\left(\frac{\mu_0 S}{t}\right)^3$
$H_r = -\frac{Mr}{128\pi}\left(\frac{\sigma_2\mu_0}{t}\right)^2$	$H_r = -\frac{3Mr}{64\pi}\left(\frac{\mu_0 S}{t}\right)^4$

Thus, measurements by a system with the transmitter-receiver separation progressively increasing at each run (Morozova et al., 1988) can provide signal increase at the respective time or response (apparent resistivity curve, ρ_τ) lengthening. The idea of successive separation increase is that the respective segments of the ρ_τ^0 curve, which is an envelope of the ρ_τ curve family, generally correspond to the highest field components, which improves the resolution relative to far-field soundings and the depth penetration relative to the near-field acquisition. The time-dependent changes in the ρ_τ^0 geometry reflect the depth-dependent changes of the subsurface properties and is independent of separation at the highest values of the field components, thus improving the resolution.

Below we discuss the potentialities of the method to measure the magnetic field. The use of magnetic sensors may be advantageous over the classical inductive loops in 2D arrays. The efficiency obviously depends on the magnetometer parameters (frequency response, time interval corresponding to high measurement accuracy, and sensitivity, i.e., the lowest measurable signal).

We performed forward modeling for a combined system consisting of a dc SQUID unit (Chwala et al., 2001) with a time range of 0.10 to 1000 ms and a magnetic variometer (Krotevich, 1972) measuring the transient magnetic field at times from 100 ms. The maximum time depended on the instrument sensitivity, which was $2.5\cdot10^{-6}$ A/m; the lowest measurable field was $H_{min} = 10^{-5}$ A/m, and the measurement accuracy was 10% (10^{-5} A/m $\cong 1.3\cdot10^{-2}$ nT).

Numerical modeling for responses typical of the Siberian craton area gave the following resistivity pattern (Agafonov, 2005; Kondrat'ev et al., 2004):

We obtained two physical-geological models for the Siberian craton: with and without an oil reservoir (models 1 and 2, respectively). Model 2 corresponded to the setting of the Angara-Lena step and included seven resistivity layers lying over a highly resistive (~2000 Ohm·m) basement.

Model 1, with a subsalt reservoir, had the same resistivities and thicknesses of the layers. The reservoir at a depth of 2200 m had a conductance of 10 S, consistent with the conditions of the Kovykta gas-condensate field.

The objective was to choose and substantiate the best efficient way of detecting a reservoir with a resistivity of 1 Ohm·m and a thickness of 10 m lying at a depth of 2200 m.

Galvanic systems

We investigated the magnetic field of a horizontal electric dipole (I_x, with a moment of $2\cdot10^5$ A·m) beginning with the behavior of the current-parallel horizontal component H_x, at $\varphi = 45°$.

We compared the two models, with (model 1) and without (model 2) a reservoir (Fig. 1), for transmitter-receiver separations of 2, 4, and 6 km and a lowest measurable signal of $H_{min} = 10^{-5}$ A/m (marked by vertical bars in the resistivity curves). A series of measurements at different separations gave responses with a long ascending branch (from 0.06 to 0.2 s), and thus provided more accurate layer conductance and thickness estimates. The field at 0.2 s was $2\cdot10^{-7}$ A/m at a separation of 2 km and $6\cdot10^{-6}$ A/m at $r = 6$ km. The reservoir was the most prominent (field difference exceeding 40%) in the zone S beginning from the curve minimum at a large separation.

Then we studied the behavior of the vertical component H_z at late times, at separations same as for the horizontal component but $\varphi = 90°$. The measurement time was twice as long as in the horizontal component (Fig. 2). The section was the best resolved at separations of 2 to 6 km, with regard to the frequency response of the system. The H_z difference between the two models (1 and 2, with and without a reservoir, respectively) exceeded 40% at the ρ_τ minimum, at a large separation. Note that the H_z component decayed more slowly and had a greater amplitude than the horizontal component at

Model 1		
Layer	ρ, Ohm·m	h, m
1	200	200
2	20	300
3	250	600
4	500	1100
5	1	10
6	300	500
7	2000	∞

Model 2		
Layer	ρ, Ohm·m	h, m
1	200	200
2	20	300
3	250	600
4	500	1100
5	300	500
6	2000	∞

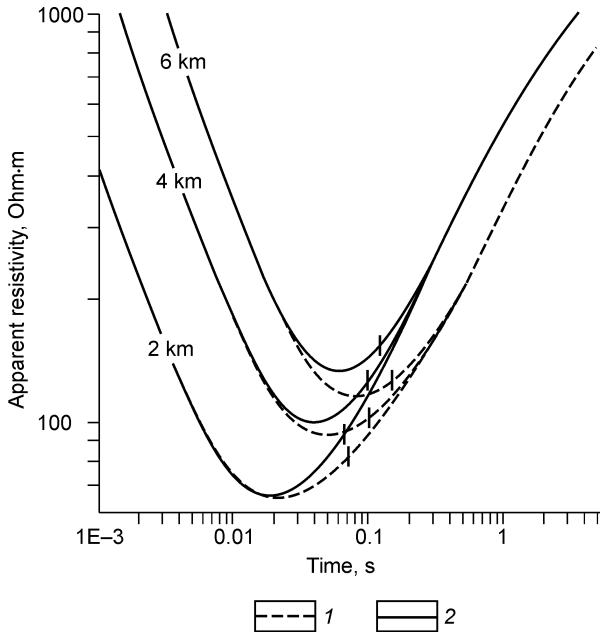

Fig. 1. Measurement system $I_x - H_x$. *1* — model 1; *2* — model 2. Symbols of curves are keyed according to transmitter-receiver separation. Vertical bar marks magnetometer's sensitivity limit ($H_x = 10^{-5}$ A/m).

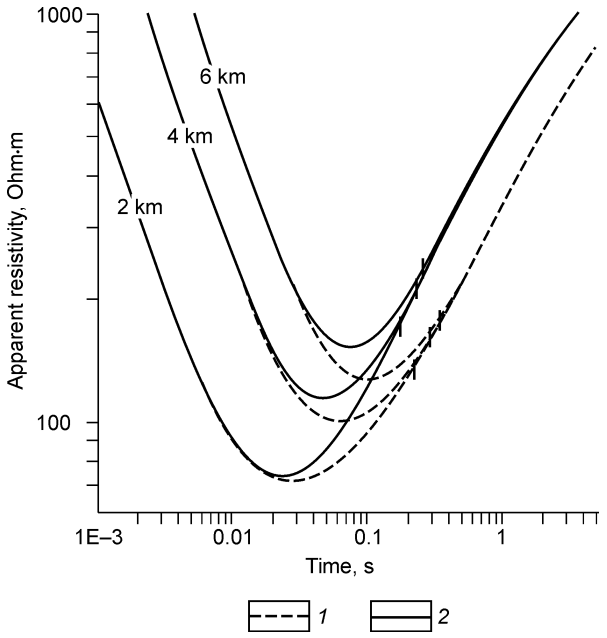

Fig. 2. Measurement system $I_x - H_z$. *1* — model 1; *2* — model 2. Symbols of curves are keyed according to transmitter-receiver separation. Vertical bar marks magnetometer's sensitivity limit ($H_z = 10^{-5}$ A/m).

late times. See Table 2 for the H_x and H_z components and their ratios at times corresponding to the $\rho\tau$ minimum.

Another experiment addressed the behavior of loop transient responses for a receiver with a moment of 8100 m^2 and $\varphi = 90°$.

Unlike the previous systems, the $\rho\tau$ minimum in this one corresponded to the transition from the wave zone where the responses decayed exponentially with distance to the late-time pattern where they were proportional to the distance. At the $\rho\tau$ minimum the responses were low sensitive to the presence of a reservoir while the signal was low (hundreds of microvolt) at the times where the patterns with and without the reservoir were distinguishable.

Thus, measuring the TEM field rather than its derivatives appears to be preferable to detect deep reservoirs.

More experiments were applied to test the depth resolution of the H_x component for a horizontal electric dipole (I_x — H_x) using a model with a deeper (2700 m) reservoir simulated by setting a thicker fourth layer (1600 m instead of 1100 m). The $\rho\tau$ curves for a series of separations (Fig. 3) had their ascending branches extended to later times, the $\rho\tau$ minimum corresponded to a rather high filed of $2–20\cdot10^{-5}$ A/m. See the times corresponding to 10^{-5} A/m and a 30% anomaly produced by a reservoir at times later than 0.1 s. Thus, the 500 m deeper reservoir remained resolvable.

Another model (Model 3) included a thinner (5 m) and, correspondingly, less conductive reservoir with its conductance (S_{rsv}) 0.25 that of the overburden (S_{ovrbd}).

The H_x components computed for models 1 and 3 are compared in Table 3 showing the H_x component at the $\rho\tau$ minimums corresponding to lowest measurable signals (Fig. 1) and the H_x ratios of the two models ($H_x^{(3)}/H_x^{(4)}$), at r = 6 km.

The $\rho\tau$ minimums mainly corresponded to signals above the magnetometer sensitivity. The $H_x^{(3)}/H_x^{(4)}$ ratios varied from 1.0 at early times, when the reservoir was unresolved, to 0.5 at late times where $H_x^{(3)}/H_x^{(4)} = (S_2/S_3)^4 \approx 0.5$ (S_1 and S_2 are the conductances in sections 1 and 2, respectively). The anomaly reached 40% at times where the response was equal to or lower than the instrument sensitivity (Fig. 1 and Table 3).

We set an electric dipole moment of $I_x = 2\cdot10^5$ A·m assuming an amperage of 100 A. This amperage is hard to maintain in a grounded line because of a high grounding resistance. Yet, one can measure a signal equal to the magnetometer sensitivity (if it is $2.5\cdot10^{-6}$ A/m) using charge storage, which allows reducing the transmitter amperage and the respective energy costs during the surveys.

Table 2

t, s	H_z	H_z	H_z/H_x	H_z/H_x
	r = 2 km	r = 6 km	r = 2 km	r = 6 km
0.011	$1.8\cdot10^{-3}$	$2.4\cdot10^{-4}$	3.3	2.0
0.109	$4.9\cdot10^{-5}$	$9.6\cdot10^{-5}$	13.5	6.7
0.503	$1.5\cdot10^{-6}$	$5.5\cdot10^{-6}$	42.3	21.1

Table 3

Component	t, s				
	0.011	0.021	0.041	0.079	0.10
$H_x^{(3)}$, $H_x^{(1)}$	$2.8\cdot10^{-4}$	$2.1\cdot10^{-4}$	$1.2\cdot10^{-4}$	$4.3\cdot10^{-5}$	$2.2\cdot10^{-5}$
$H_x^{(3)}/H_x^{(1)}$	1.0	0.99	0.92	0.85	0.78

Model 3

Layer	ρ, Ohm·m	*h*, m
1	200	200
2	20	300
3	250	600
4	500	1100
5	1	5
6	300	500
7	2000	∞

Inductive systems

A classic inductive measurement system with horizontal transmitter and receiver loops, i.e., purely inductive excitation, was simulated assuming a transmitter moment of $3.6 \cdot 10^7$ A·m^2 and a receiver moment of 8100 m^2. Computing for models 1 and 2 at a separation of $r = 1$ km gave a 23 μV signal at the time corresponding to the ρ_τ minimum. However, the reservoir became prominent only at late times where the signal was less than 1 μV. The responses were independent of separation.

Another case we simulated in the context of the suggested method was excitation by a vertical magnetic dipole and measurements of the radial magnetic field component, at the same dipole moment as in the previous model. The radial component of the magnetic field was proportional to the separation r at late times and decreased exponentially (r^3) at early times. The reservoir showed up after the ρ_τ minimum for $r > 4$ km. The anomaly was 30% at the ρ_τ minimum, at the lowest measurable signal of $1.5 \cdot 10^{-5}$ A/m. Thus, inductive measurements of the magnetic field at successively increasing separations can likewise be advantageous or more informative in this case.

The section of the Siberian craton may contain several reservoirs, and it is pertinent to investigate the problem of their discrimination in galvanic and inductive data.

We performed modeling for two resistivity patterns, with one and two reservoirs (models 4 and 5, respectively), with the aim to discriminate the responses of two reservoirs lying at depths of 1800 m and 2200 m. See the behavior of the H_x component as a function of separation and number of reservoirs in Fig. 4. Measurements at a series of increasing separations were obviously advantageous because the responses at a small separation of $r < 2$ km resolved only the upper reservoir while the field at the ρ_τ minimum was indifferent to the properties of the lower reservoir. The anomaly produced by the other reservoir appeared at a greater separation. The radial magnetic field component plotted in the vicinities of the first and second minimums (Fig. 4) did not show the late-time pattern near the first ρ_τ minimum and, hence, the field was maximum at the short separation.

Discrimination between two reservoirs was investigated for a high resolution system of an electric dipole and a horizontal loop. As in the previous models, we assumed a transmitter moment of $I_x = 2.5 \cdot 10^5$ A·m and a receiver moment of 8100 m^2. The effect of reservoirs appeared as two ρ_τ minimums at a high signal, with a response of 147 μV at the first minimum. The signal was from tens to a few microvolt near the minimum at $t < 0.3$ (Fig. 5). According to (2), the response increases with separation, but this occurs at $t > 0.5$ s where the signal is fractions of μV.

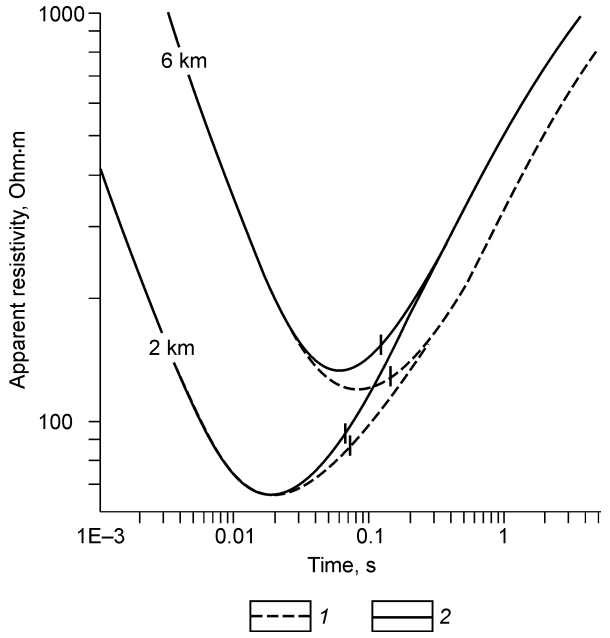

Fig. 3. Measurement system $I_x - H_x$. *1* — model 1; *2* — model 2, with a deep reservoir. Symbols of curves are keyed according to transmitter-receiver separation. Vertical bars mark magnetometer's sensitivity limit ($H_x = 10^{-5}$ A/m).

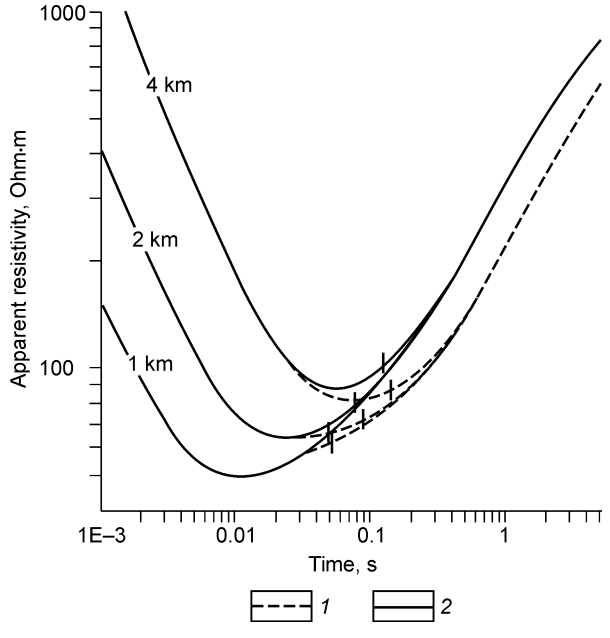

Fig. 4. Discriminating responses of two reservoirs in system $I_x - H_x$. *1* — one reservoir; *2* — two reservoirs. Symbols of curves are keyed according to transmitter-receiver separation. Vertical bars mark magnetometer's sensitivity limit ($H_x = 10^{-5}$ A/m).

Model 4		
Layer	ρ, Ohm·m	*h*, m
1	200	200
2	20	300
3	250	600
4	500	700
5	1	10
6	300	500
7	2000	∞

Model 5		
Layer	ρ, Ohm·m	*h*, m
1	200	200
2	20	300
3	250	600
4	500	1100
5	1	10
6	500	400
7	1	10
8	300	500
9	2000	∞

Conclusions

Mathematical modeling of the systems $I_x - H_x$, $I_x - H_z$, $I_x - \partial B_z/\partial t$, $M_z - H_r$, $M_z - H_z$, $M_z - \partial B_z/\partial t$ was applied to

— detect reservoirs lying at different depths;

— detect a reservoir at different reservoir/overburden conductance ratios;

— discriminate the responses of two reservoirs lying at different depths.

The numerical experiments confirmed the advantage of TEM-TDEM soundings with successively increasing separations which provide a better resolution and a greater penetration depth.

The advantage was especially notable in galvanic current systems. However, galvanic data may be more strongly affected by the crust heterogeneity than inductive data because the electromagnetic field of electric dipoles bears the electric mode. This issue will be a subject of a special 3D modeling study.

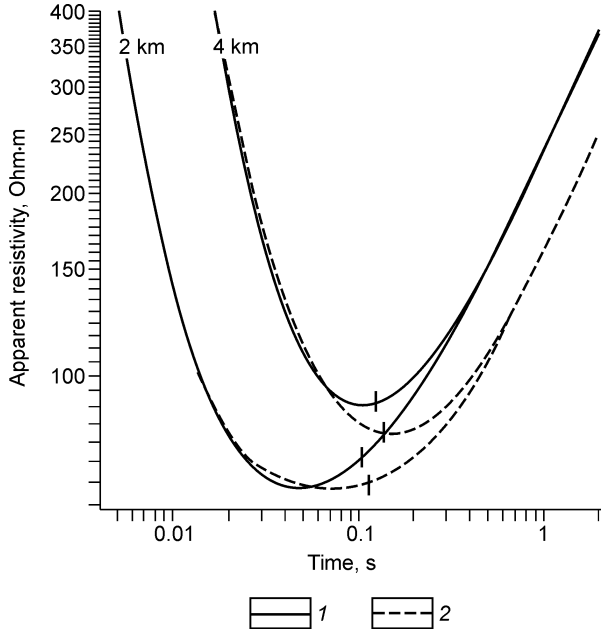

Fig. 5. Discriminating responses of two reservoirs in system $I_x - Q$. Symbols of curves are keyed according to transmitter-receiver separation. Vertical bars mark magnetometer's sensitivity limit. *1* — model 4 (one reservoir), *2* — model 5 (two reservoirs).

References

Agafonov, Yu.A., 2005. Designing a TEM acquisition-processing system for telemetric soundings [in Russian]. Author's Abstract, Candidate Thesis, Novosibirsk.

Agafonov, Yu.A., Pospeev, A.V., 2001. A near-field TEM acquisition-processing system. Geofizicheskii Vestnik, No. 10, 8–11.

Barsukov, P.O., Fainberg, E.B., Khabenskii, E.O., 2002. The TEM-FAST electromagnetic technology for sounding the subsurface, in: Spichak, V.V. (Ed.), Geological Interpretation of Gravity, Magnetic, and Electric Fields: Theory and Practice [in Russian]. IOFZ RAN, Moscow, pp. 20–21.

Chwala, A., Schultze, V., Stolz, R., Jsselsteijn, R.I., Meyer, H.-G., Kretzschmar, D., 2001. An HTS dc SQUID system in competition with induction coils for TEM applications. Physica C 354, 45–48.

Epov, M.I., Dashevskii, Yu.A., Yel'tsov, I.N., 1990. Machine-Aided Processing of EM Data [in Russian]. Preprint, IGiG SO AN SSSR, No 3, Novosibirsk.

Epov, M.I., Yel'tsov, I.N., 1992. Forward and Inverse 1D TEM Problems [in Russian]. Preprint, OIGGM SO RAN, No 2, Novosibirsk.

Kaufman, A.A. (Ed.), 1971. Near-field TEM Soundings [in Russian]. Preprint, SO AN SSSR, IGiG, Novosibirsk.

Kaufman, A.A., Morozova, G.M., 1970. The Near-Field TEM Soundings: Theoretical Background [in Russian]. Nauka, Novosibirsk.

Kondrat'ev, V.A., Pospeev, A.V., Agafonov, Yu.A., Pashevin, A.M., Ol'hovik, E.A., 2004. New technologies of TEM soundings in the southern Siberian craton. Razvedka and Okhrana Nedr, Nos. 8–9, 26–28.

Krotevich, N.F., 1972. Microvariation Magnetic Soundings and MTS Instruments [in Russian]. Nauka, Novosibirsk.

Mandel'baum, M.M., Rabinovich, B.I., Surkov, B.C., 1980. Direct geophysical methods for petroleum prospecting (example of the Siberian Platform), in: Trofimuk, A.A. (Ed.), Scientific Heritage of Academician I.M. Gubkin in Petroleum Geology of Siberia [in Russian]. Nauka, Novosibirsk, pp. 48–73.

Morozova, G.M., Sokolov, V.P., Nevedrova, N.N., 1988. A Method of Electromagnetic Soundings [in Russian]. Author's Certificate 1500127 (USSR), MKI GO 1V3/108. BI Publ., 1988, No 29.

Toropov, S.M., Man'kovskii, A.G., 2004. Information Systems for assessment, monitoring, and use of mineral resources. Razvedka and Okhrana Nedr, Nos. 8–9, 36–39.

Trigubovich, G.M., Zaharkin, A.K., Mogilatov, B.C., 1990. The TEM method: A technological complex, in: Electromagnetic Induction in the Upper Crust [in Russian]. Nauka, Moscow, pp. 155–156.

Zakharkin, A.K., 1981. Methodological Guidelines for the Use of the Tsikl TEM system [in Russian]. SNIIGGiMS, Novosibirsk.

Editorial responsibility: M.I. Epov